CHANGE OF THE ELECTRON EFFECTIVE MASS IN EXTREMELY HEAVILY DOPED n-TYPE SI OBTAINED BY ION IMPLANTATION AND LASER ANNEALING

M. Miyao, T. Motooka, N. Natsuaki and T. Tokuyama

Central Research Laboratory, Hitachi Ltd., Kokubunji, Tokyo 185, Japan

(Received 23 July 1980 by W. Sasaki)

Infrared optical properties of extremely heavily doped n-type Si, obtained by ion implantation and laser annealing, were studied. A new relation between free carrier effective mass (m^*) and carrier concentration $(10^{19}-5\times10^{21}\,\mathrm{cm}^{-3})$ was obtained. The value of m^* increases significantly with the increase of carrier concentration, when carrier concentration exceeds $10^{21}\,\mathrm{cm}^{-3}$. The result is discussed in relation to the occupation of electrons in a new valley of the conduction band.

1. INTRODUCTION

OPTICAL PROPERTIES of free electrons in doped semiconductors have been investigated by many researchers [1], because they provide information concerning the conduction band. The pioneering work of Spitzer and Fan [2] indicated that the electron effective mass (m^*) can be determined by measuring the dielectric function. Since then, free electron absorption [3] and plasma reflectivity [4-6] experiments have been used to determine m^* and also to evaluate the doping homogeneity of semiconductor crystals.

These results indicate that the values of m^* change with energy above the conduction band, particularly, an increase of m^* due to impurity doping was observed in InSb [2] and GaAs [3]. However, in the case of Si, a significant change in m^* has not been reported. The reason for this is that in Si the density of states of the conduction band edge is large and the non-parbolicity is small compared with InSb and GaAs. Therefore, extremely heavy doping is necessary to observe the effective mass change in Si.

Recently, new doping technique, i.e. ion implantation and laser annealing [7] has been developed. This makes it possible to dope Si with electrically active impurities to the level which significantly exceeds the thermal equilibrium solid solubility. The maximum peak carrier concentration is reported as 5×10^{21} cm⁻³, which is higher by an order of magnitude than previous experiments [1].

The present paper describes the infrared optical properties of ion implanted and laser annealed Si. An appreciable change of m^* is found in externely heavily doped Si.

2. EXPERIMENTS

Several p-type (100) Si wafers with 10Ω -cm resistivities were implanted by phosphorus (P) ions (50 keV)

or arsenic (As) ions (80 keV) at doses of 6×10^{14} to 5×10^{16} cm⁻², followed by *Q*-switched pulse ruby laser annealing (laser wavelength = $0.6943 \, \mu \text{m}$, pulse duration time = $25 \, \text{nsec}$, energy density = $0.5 - 1.5 \, \text{J cm}^{-2}$).

Carrier concentration profiles were determined by a combination of Hall effect measurement and the conventional anodic oxidation layer removal method. Optical reflection and transmission were measured using a DIGILAB FTS-20 spectrometer in the spectral region of $400-1200 \text{ cm}^{-1}$ at 300 K.

3. RESULTS AND ANALYSIS

3.1. Heavy doping by ion implantation and laser annealing

Surface carrier concentration (number of carriers per square centimeter) and carrier concentration (number of carriers per cubic centimeter) profile after ion implantation and laser annealing were measured as a function of laser energy. Implantation induced amorphous layers were completely recrystallized and all implanted ions were electrically activated when laser energy exceeded 1.0 J cm⁻². Implanted atoms spread as laser energy increased, and, at 1.5 J cm⁻² irradiation, carrier concentration profiles showed flat profiles.

Typical results are shown in Fig. 1, where calculated P atom profiles before laser annealing are also shown. Peak carrier concentration is 1×10^{21} and 5×10^{21} cm⁻³ for 1×10^{16} and 5×10^{16} P⁺ cm⁻² implanted samples, respectively. These values well exceed the limit of thermal equilibrium solid solubility $(1.3\times10^{21}\,\mathrm{cm^{-3}})$ of P atoms in Si [8] because melting and subsequent rapid cooling $(10^{10}\,\mathrm{deg\,sec^{-1}})$ are caused by laser annealing [7]. In addition, transmission electron microscopy observation confirmed that no extended defect is observed after laser annealing $(1.0-1.5\,\mathrm{J\,cm^{-2}})$.

Thus, extremely heavy doping of impurities

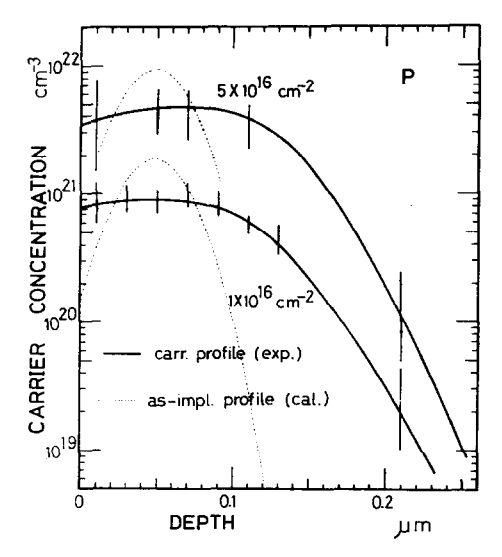


Fig. 1. Carrier concentration profiles after P⁺ implantation and laser annealing. Dashed lines represent calculated impurity profiles. Vertical lines indicate probable experimental errors.

(≥ 10²¹ cm⁻³) without macroscopically extended defects is realized by high dose ion implantation and laser annealing. Thus, 1.5 J cm⁻² was chosen as the standard laser energy for experimental condition.

3.2. Determination of effective mass

Optical measurements were performed to determine free electron effective mass in the ion implanted and laser annealed layer. The carrier concentration (N) dependence of reflectivity is shown in Fig. 2(a), where N is the peak carrier concentration as shown in Fig. 1. The wavenumber $(1/\lambda_{\min})$ at which reflectivity shows

minimum value shifts to the higher wavenumber with the increase of carrier concentration. The values of $1/\lambda_{\min}$ for $P^+(\bullet)$ or $As^+(\blacktriangle)$ implanted samples are summarized as a function of N in Fig. 2(b). In the figure, previously reported results [2, 5, 6] for P atom doped samples $(\square, \bigcirc, \triangle)$ are also shown.

The values of m^* were determined from the relationship [2]

$$\left(\frac{1}{\lambda_{\min}}\right)^2 = \frac{e^2}{\pi c^2 (\epsilon_{\infty} - 1) m^*} N \tag{1}$$

where ϵ_{∞} is the dielectric constant of non-doped crystal, c is the light velocity and e is the electron charge. The same effective masses of $0.28m_0$ (m_0 ; the electron rest mass) were obtained in the carrier concentration region below 10^{21} cm⁻³. However, when the carrier concentration exceeds 10^{21} cm⁻³, m^* increases with the increase in carrier concentration, i.e. values of $0.45m_0$ and $0.55m_0$ are obtained for doping levels of 3×10^{21} cm⁻³ and 5×10^{21} cm⁻³, respectively. These values are the same for different dopants, such as P and As, so stress is not the main factor influencing effective mass.

Equation (1) is valid under the condition of $\omega \tau > 1$, where ω is the angular frequency of the incident light and τ is the carrier relaxation time. However, the value of τ in the extremely heavily doped layer is not known. Thus, the results should be examined carefully.

In order to obtain values of both m^* and τ , free carrier absorption was measured in the infrared region. Transmission spectra are shown in Fig. 3 as a function of carrier concentration.

These results were analyzed as follows; first, the transmittance (T) was calculated using the two layer

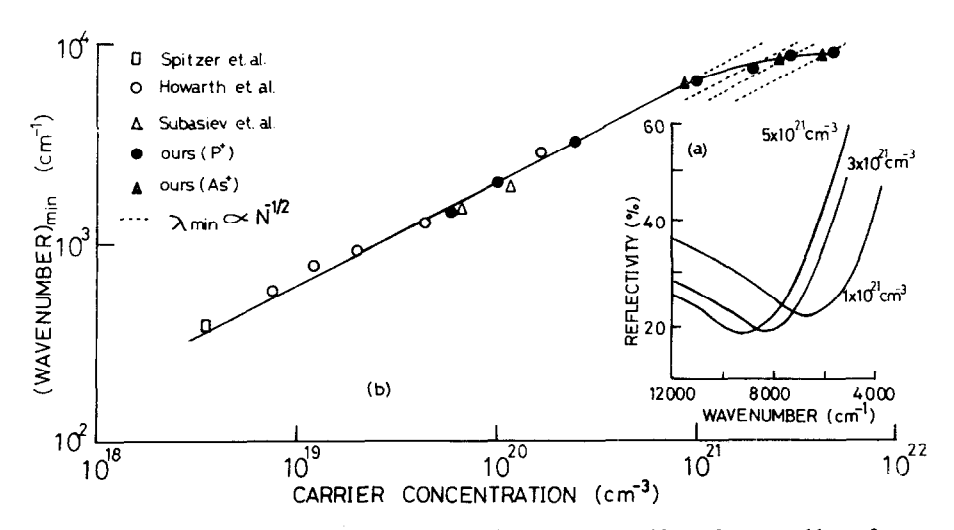


Fig. 2. (a) Reflectivity spectra after P^+ implantation (1 × 10¹⁶ cm⁻², 3 × 10¹⁶ cm⁻², 5 × 10¹⁶ cm⁻² at 50 keV) and laser annealing (1.5 J cm⁻²). Peak carrier concentrations for each samples are listed in the figure. (b) The relations between carrier concentration and wavenumbers where the reflectivity shows minimum values.

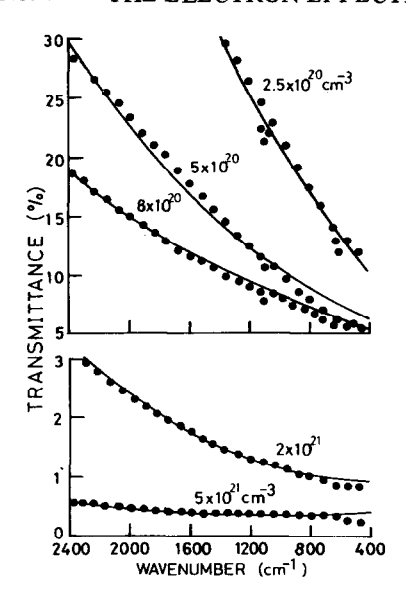


Fig. 3. Infrared transmission spectra after P^+ implantation (50 keV for 2.5×10^{15} , 5×10^{15} , 8×10^{15} , 2×10^{16} , $5 \times 10^{16} \, \text{cm}^{-2}$) and laser annealing (1.5 J cm $^{-2}$). Peak carrier concentrations for each sample are listed in the figure. Calculated transmission spectra are shown as solid lines.

model, i.e. the homogeneously heavy doped layer and the substrate layer. The final form of T [9] became,

$$T = \left| \frac{(1 - r_1^2)(1 - r_2^2)e^{i\gamma_1}}{[1 - r_1(r_1 - r_2)e^{2i\gamma_1} - r_1r_2]} \right|^2 \times \frac{e^{-\alpha_2 d_2}}{1 - |Q|^2 e^{-2\alpha_2 d_2}},$$

where

$$Q = -\frac{r_2[r_1 - r_2 + r_1(r_1r_2 - 1)e^{2i\gamma_1}]}{1 - r_1^2e^{2i\gamma_1} + r_1r_2(e^{2i\gamma_1} - 1)},$$

$$r_i = \frac{\sqrt{\epsilon_i} - 1}{\sqrt{\epsilon_i} + 1},$$

$$\gamma_i = \frac{2\pi d_i\sqrt{\epsilon_i}}{r_i},$$

$$\sqrt{\epsilon_i} = n_i + ik_i$$

(i=1 for the doped layer and i=2 for the substrate), n_i is the refractive index, k_i is the extinction coefficient, α_i (= $4\pi k_i/\lambda$) is the absorption constant and d_i is the layer thickness. Drude type dielectric function

$$\epsilon(\omega) = \epsilon_{\infty} - \frac{4\pi N e^2}{m^* \omega^2} \frac{1}{1 + i(1/\omega \tau)}$$

was employed for the analysis. Then, data fitting was done by choosing m^* and τ as the fitting parameters. The other parameters $(N, d, \epsilon_{\infty})$ were the measured values.

Calculated transmission spectra are shown in Fig. 3 with solid lines. They agree well with experimental results. The determined values of τ (\blacktriangle) are shown in Fig. 4. Carrier relaxation time decreases slightly with the increase of carrier concentration. The lowest value of τ is 3×10^{-15} sec, so the condition of $\omega \tau > 1$ was fulfilled for all samples. Thus, the validity of the method to obtain m^* from optical reflectivity is proved.

In the figure, the values of m^* (\bullet) derived from Fig. 3 are compared with that (\circ) obtained from Fig. 2. The same relation between m^* and N was obtained by different methods, i.e. optical reflection and transmittance, for different spectral regions.

4. DISCUSSION

Recently, Chelikowski and Cohen [10] calculated the Si band structure. Results indicated that a valley with a heavier effective mass exists on the X-U line about 0.2 eV above the conduction band minimum. Carrier concentration at which Fermi level enter a new valley is $5 \times 10^{20} \, \mathrm{cm}^{-3}$. This value is close to the carrier concentration at which m^* begins to increase.

Thus, the change in m^* can be explained as the result of entrance into a new valley of electrons which have overflown the conventional valley on the $\Gamma - X$ line. In addition, non-parabolicity of the conventional

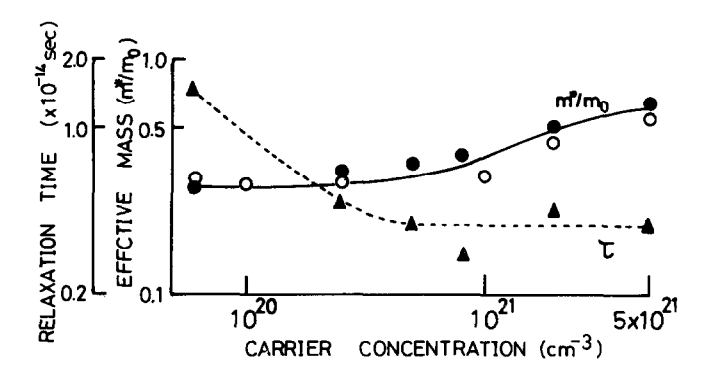


Fig. 4. Carrier concentration dependence of free electron effective mass (m^*) and carrier relaxation time (τ) .

conduction band is found to be small in the energy region up to 0.2 eV from the conduction band minimum.

More precise calculation of the conduction band, including calculation of the impurity potential effect, is now underway.

REFERENCES

- R.A. Abram, G.J. Ress & B.L.H. Wilson, Adv. Phys. 27, 799 (1978).
- 2. W.G. Spitzer & H.Y. Fan, *Phys. Rev.* 106, 882 (1957).
- W.G. Spitzer & J.M. Whelan, Phys. Rev. 114, 59 (1959).

- 4. E.E. Gardner, W. Kappallo & C.R. Gordon, *Appl Phys. Lett.* **9**, 432 (1966).
- 5. L.E. Howarth & J.F. Gilbert, J. Appl. Phys. 34, 236 (1963).
- 6. V.K. Subashiev, G.B. Dubrovskii & A.A. Kukharskii Sov. Phys. Solid State 6, 830 (1964).
- 7. Proc. Laser-Solid Interactions and Laser Processing (1978); (Edited by S.D. Ferris, H.J. Leamy & J.M. Poate). American Inst. Phys., N.Y. (1979).
- 8. F.A. Trumbore, Bell Syst. Tech. J. 39, 205 (1960).
- 7. Motooka, M. Miyao & T. Tokuyama (unpublished).
- J.R. Ćhelikowsky & M.L. Cohen, *Phys. Rev.* B14, 556 (1976).